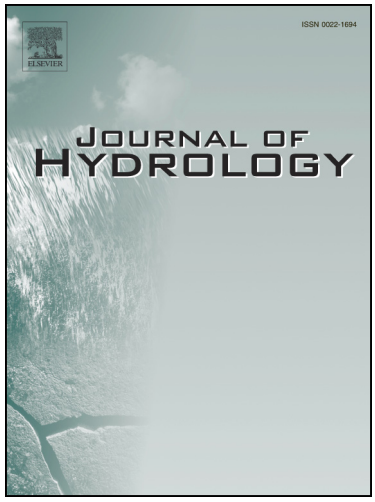

Controls of groundwater floodwave propagation in a gravelly floodplain

Claude-André Cloutier, Thomas Buffin-Bélanger, Marie Larocque

PII: S0022-1694(14)00111-5
DOI: http://dx.doi.org/10.1016/j.jhydrol.2014.02.014
Reference: HYDROL 19405

To appear in: *Journal of Hydrology*

Received Date: 30 October 2013
Revised Date: 24 January 2014
Accepted Date: 3 February 2014

Please cite this article as: Cloutier, C-A., Buffin-Bélanger, T., Larocque, M., Controls of groundwater floodwave propagation in a gravelly floodplain, *Journal of Hydrology* (2014), doi: http://dx.doi.org/10.1016/j.jhydrol.2014.02.014

Controls of groundwater floodwave propagation in a gravelly floodplain

Claude-André Cloutier
Département de biologie, chimie et géographie, Centre for Northen Studies (CEN)
Université du Québec à Rimouski
Rimouski, QC, Canada, G5L 3A1
Phone : 418-723-1968 # 1733
Claude-andre_Cloutier@uqar.ca

Thomas Buffin-Bélanger
Département de biologie, chimie et géographie, Centre for Northen Studies (CEN)
Université du Québec à Rimouski
Rimouski, QC, Canada, G5L 3A1
Phone : 418-723-1968 # 1577
Thomas_Buffin-Belanger@uqar.ca

Marie Larocque
Département des sciences de la Terre et de l'atmosphère
Université du Québec à Montréal
C.P. 8888 succursale Centre-ville, Montréal, QC, Canada
H3C 3P8
Phone: 514-987-3000 # 1515
larocque.marie@uqam.ca

Key Points:

- A groundwater floodwave can propagate through an alluvial aquifer
- Streamfloods affect groundwater flow orientation
- Streamfloods leading to groundwater exfiltration

Index Terms: Groundwater; Floodplain dynamics; Groundwater – surface water interaction; Floods

Key words: river–groundwater interactions; flood events; groundwater flooding; groundwater floodwave; flow reversals; floodplain; Matane River (eastern Canada)

ABSTRACT

Interactions between surface water and groundwater can occur over a wide range of spatial and temporal scales within a high hydraulic conductivity gravelly floodplain. In this research, dynamics of river-groundwater interactions in the floodplain of the Matane River (eastern Canada) are described on a flood event basis. Eleven piezometers equipped with pressure sensors were installed to monitor river stage and groundwater levels at a 15-minutes interval during the summer and fall of 2011. Results suggest that the alluvial aquifer of the Matane Valley is hydraulically connected and primarily controlled by river stage fluctuations, flood duration and magnitude. The largest flood event recorded affected local groundwater flow orientation by generating an inversion of the hydraulic gradient for sixteen hours. Piezometric data show the propagation of a well-defined groundwater floodwave for every flood recorded as well as for discharges below bankfull (< 0.5 Qbf). A wave propagated through the entire floodplain (250 m) for each measured flood while its amplitude and velocity were highly dependent on hydroclimatic conditions. The groundwater floodwave, which is interpreted as a dynamic wave, propagated through the floodplain at 2-3 orders of magnitude faster than groundwater flux velocities. It was found that groundwater exfiltration can occur in areas distant from the channel even at stream discharges that are well below bankfull. This study supports the idea that a river flood has a much larger effect in time and space than what is occurring within the channel.

64

65 1. INTRODUCTION

66 A gravel-dominated floodplain and its fluvial system are hydrologically connected
67 entities linked by interactions beyond recharge and discharge processes. Woessner (2000)
68 emphasized the need to conceptualize and characterize surface-water–groundwater
69 exchanges both at the channel and at the floodplain scale to fully understand the complex
70 interactions between the two reservoirs. The stream-groundwater mixing zone is referred
71 to as the hyporheic zone. It is generally understood that surface water-groundwater
72 mixing exchanges at channel and floodplain scales are driven by hydrostatic and
73 hydrodynamic processes, the importance of which varies according to channel forms and
74 streambed gradients (Harvey and Bencala, 1993; Stonedahl et al., 2010; Wondzell and
75 Gooseff, 2013). The boundaries of the hyporheic zone can be defined by the proportion
76 of surface water infiltrated within the saturated zone (Triska et al., 1989) or by the
77 residence time of the infiltrated surface water (Cardenas, 2008; Gooseff, 2010). However,
78 pressure exchanges between surface water and groundwater can occur beyond the
79 hyporheic zone, with no flow mixing (Wondzell and Gooseff, 2013). River stage
80 fluctuations can lead to the generation of groundwater flooding via pressure exchanges.
81 Groundwater flooding, i.e., groundwater exfiltration at the land surface, is controlled by
82 several factors in floodplain environments: floodplain morphology, pre-flooding depth of
83 the unsaturated zone, hydraulic properties of floodplain sediments, and degree of
84 connectivity between the stream and its alluvial aquifer (Mardhel et al., 2007). Two
85 scenarios can lead to the rise of groundwater levels resulting in flooding: 1) the complete
86 saturation of subsurface permeable strata due to a prolonged rainfall and 2) groundwater

level rises due to river stage fluctuations. Concerning the second scenario, Burt et al. (2002) and Jung et al. (2004) noted that once the River Severn (UK) exceeded the elevation of the floodplain groundwater in summer conditions, the development of a groundwater ridge was responsible for switching off hillslope inputs at stream discharges below bankfull. Mertes (1997) also illustrated that inundation of a dry or saturated floodplain may occur as the river stage rises, even before the channel overtops its banks. In-channel and overbank floods perform geomorphic work that modifies groundwater-surface water interactions (Harvey et al., 2012). In contrast, groundwater floodwaves propagation performs no geomorphic work, but nevertheless can influence riparian ecology or flooding of humanbuilt systems on floodplains (Kreibich and Thieken, 2008).

Field studies at the river-reach scale have been carried out to document the hydrological interactions between river stage and groundwater fluctuations beyond the hyporheic zone in floodplain environments (e.g., Burt et al., 2002; Jung et al., 2004; Lewandowski et al., 2009; Vidon, 2012). It has been reported that river stage fluctuations were responsible for delayed water level fluctuations at distances greater than 300 m from the channel (e.g., Verkerdy and Meijerink, 1998; Lewandowski et al., 2009). The process of pressure wave propagation through the floodplains (Sophocleous, 1991; Verkerdy and Meijerink, 1998; Jung et al., 2004; Lewandowski et al., 2009; Vidon, 2012) and the direction of exchanges between groundwater and surface water at the river bed (Barlow and Coupe, 2009) have has also been documented. However, only a few field studies describe the interactions between surface water and groundwater on a flood event basis (e.g., Burt et al., 2002; Jung et al., 2004; Barlow and Coupe, 2009; Vidon, 2012). Moreover, field

instrumentation usually covers only a limited portion of the floodplain with transects of piezometers (Burt et al., 2002; Jung et al., 2004; Lewandowski et al., 2009). The lack of empirical data on the propagation of groundwater flooding in two dimensions during several flood events limits our understanding of complex river-groundwater interactions. Using higher spatial and temporal resolutions is necessary to describe how flow orientations within alluvial floodplains are affected by flood events. Furthermore, the processes that generate groundwater exfiltration and the effects of floodplain morphology on river-groundwater interactions in alluvial floodplains need to be better understood to facilitate land use management in floodplains.

The aim of this paper is to document surface water-groundwater interactions in an alluvial floodplain at high spatial and temporal resolutions at the flood event scale. The study was carried out on the Matane River floodplain (province of Quebec, Canada). The Matane Valley is known to experience floods of different types every few years: overbank flow during snow melt, during rainstorms, or by ice jams. The valley is also known to experience flooding in areas that are distant from the channel when there is no overbank flow. An experimental site was instrumented and water levels were monitored for 174 days in the summer and fall of 2011. Time series analysis was used to interpret results and provide a detailed picture of the interactions between river and groundwater levels.

2. MATERIALS AND METHODS

2.1 Study site

The Matane River flows from the Chic-Choc mountain range to the south shore of the St. Lawrence estuary, draining a 1678 km^2 basin (Figure 1). The flow regime of the Matane River is nivo-pluvial, with the highest stream discharges occurring in early May. The mean annual stream discharge is 39 m^3s^{-1} (1929–2009), and the bankfull discharge is estimated at 350 m^3s^{-1}. Discharge values are available from the Matane gauging station (CEHQ, 2013; station 021601). The irregular meandering planform flows into a wide semi-alluvial valley cut into recent fluvial deposits (Lebuis, 1973). The entire floodplain of the gravel-bed Matane River is constructed by different types of meander growths that shift over time. The mean channel width and the mean valley with are 55 m and 475 m, respectively.

The study site, located 28 km upstream from the estuary (48° 40' 5.678" N, 67° 21' 12.34" W), is characterized by an elongated depression that corresponds to an abandoned oxbow and a few overflow channels (Figure 1). The site was chosen for its history of flooding at river stages below bankfull. The floodplain is very low, i.e., at bankfull discharge, the deepest parts of the depression are lower than the river water level. During the study period, the mean groundwater level at the study site is 58.8 m above mean sea level, whereas the surface elevation of the floodplain is 60.4 m above sea level, i.e., the unsaturated zone is on average 1.4 m. The sediments overlying the bedrock and forming the alluvial aquifer consist of coarse sands and gravels overtopped by a overbank sand deposit layers of variable thickness from 0.30 m at highest topographic forms to 0.75 m within abandoned channels. The unconfined alluvial aquifer thickness of is 25 m according to a bedrock borehole next to the study site.

155 *2.2 Sampling strategy*

156 To investigate hydraulic heads in the floodplain, the local groundwater flows, and the
157 stream discharge at which exfiltration occurs, an array of 11 piezometers was installed
158 (Figure 1). Arrays of piezometers have been used with success in previous studies to
159 document the surface water-groundwater interactions (e.g., Haycock and Burt, 1993; Burt
160 et al., 2002; Lewandowski et al., 2009; Vidon, 2012). Piezometers are made from 3.8 cm
161 ID PVC pipes sealed at the base and equipped with a 30 cm screens at the bottom end. At
162 every location, piezometers reached 3 m below the surface so that the bottom end would
163 always be at or below the altitude of the river bed. However, because of the surface
164 microtopography, the piezometers bottom reached various depths within the alluvial
165 aquifer. Piezometer names correspond to the shortest perpendicular distance between the
166 piezometer and the river bank. Slug tests were conducted at each piezometer, and rising-
167 head values were interpreted with the Hvorslev method (Hvorslev, 1951). Results from
168 the slug tests at each piezometer indicate that hydraulic conductivities are relatively
169 homogeneous (from 8.48×10^{-4} to 2.1×10^{-5} m s^{-1}; Table 1) and representative of coarse
170 sand to gravel deposits (Freeze and Cherry, 1979).
171
172 Data were collected from 21 June to 12 December 2011. This period correspond roughly
173 to the end of the long spring flood to the beginning of winter low flow period where flow
174 stage is influenced by the formation of an ice cover. From 21 June to 7 September 2011,
175 eight piezometers were equipped with pressure transducers (Hobo U20-001) for
176 automatic water level measurements at 15 min intervals. Three more pressure transducers
177 were added at piezometers D139, D21, and D196 starting on 7 September. Two river

stage gauges were installed on the riverbed, downstream and upstream of the study site (RSGdn and RSGup; Hobo U20-001) to monitor water levels in the Matane River every 15 minutes over the complete study period. Piezometer locations were measured using a Magellan ProMark III differential GPS. A LIDAR survey with a 24 cm resolution (3.3 cm accuracy) was used to obtain a high resolution map of topography. Precipitation was measured with a tipping bucket pluviometer located on site (Hobo RG3-M).

2.3 Data analysis

During the data collection period, water levels and river stages were never lower than the piezometer and RSGup data loggers. However, river stages at RSGdn occasionally dropped below the data logger, so time series at this location are discontinuous. The RSGdn time series was only used to analyze the 5–12 September event.

During flood events, the timing of maximum water level elevation differed between the piezometers and the river gauge. To determine the time lags between time series of river stages and piezometer water levels, cross-correlation analyses were performed. Cross-correlation analyses between time series of piezometric levels, river levels, and precipitation were also used to provide information on the strength of the relationships between input and output processes and also on the time lag between the processes. Analyses were performed with the PAST software (Hammer et al., 2001) on the times series from piezometer water levels and from the RSGup for each event. Due to the distance of only 400 m between river gauges, there was no significant lag between RSGup and RSGdn data that would cause lower lag between the surface-groundwater

using a rebuilt RSGdn time series from RSGup data. The time lag corresponds to the delay at which the maximum correlation coefficient occurred between two time series.

3. RESULTS

3.1. Cross-correlation analysis of water level fluctuations

Time series of water levels and river stages indicate a strong synchronicity of the groundwater and river systems. Figure 2 shows the time series of water levels for all piezometers and for the river stage gauge upstream (RSGup) at a 15 min interval for the period of 21 June to 12 December 2011. During this period, seven floods below bankfull discharge occurred. The largest flood took place from 5–12 September, with a maximum stream discharge of 213 $m^3 s^{-1}$ on September 6 at 2:00pm (all times are reported in local time, EDT) (60% of $Q_{bankfull}$). The six other floods ranged from 29 to 72 $m^3 s^{-1}$. The 5–12 September flood event induced water level fluctuations of 1.14 and 0.68 m at piezometers D21 and D257, respectively. Figure 2 shows river levels are always higher than hydraulic heads. This is explicated by the river stage gauge that is located 400 m upstream from the study site (RSGup). The highest water levels were usually observed at piezometers distant from the river (D223–D257) and the lowest were close to the river (D21–D25), so the Matane river is generally a gaining stream.

Figure 3 presents cross-correlation functions between river levels as input processes and groundwater levels as output processes as well as cross-correlation functions between precipitation and groundwater levels for the 2–16 July event. The results reflect the strong relationship ($r > 0.9$ at maximum correlation) between the river stage fluctuations

and the groundwater level fluctuations at every piezometer. With values ranging from 0.89 to 0.98, and 8 correlations out of 11 being higher than 0.95, the cross-correlation results suggest that groundwater levels are strongly correlated with river stage fluctuations. The precipitation–groundwater level correlations (0.2 - 0.3) are significantly lower than the river–groundwater level correlations. This gives strong evidence that the input signal from precipitation is significantly reduced by the large storage capacity of the unsaturated zone.

Time lags between inputs and outputs derived from the cross-correlation analysis reveal the spatiotemporal response of the groundwater level to the rising stream discharge or to the precipitation. For the 2–16 July event, time lags between precipitation and groundwater levels (at maximum correlation) varied from 22 to 44 hours while time lags between river stage and groundwater levels varied from 1 to 22 hours. In both cases, the shorter time lags are associated with piezometers located closer to the river. The longer precipitation-groundwater level time lags reveal a significant storage capacity of the unsaturated zone during precipitation, and the shorter river-groundwater level time lags are interpreted as an indication that groundwater fluctuations are associated with river level fluctuations.

Figure 4 shows the relationship between the time lags from the river level-groundwater level cross-correlation analysis and the piezometer distance from the river for three flood events. A strong linear relationship emerges between the two variables as shown by the

246 strong R^2 for the regression model for the three flood events (all R^2 values are higher than
247 0.91). The scatter for each event may be due to the fact that the piezometers are not
248 perfectly aligned (see Figure 1c). The figure also shows that at 250 m the highest
249 groundwater level is reached 25 h later than the highest river stage for the September
250 flood event, but 40 h later for the November flood event. This reveals contrasting
251 propagation velocities for the groundwater crest moving throughout the floodplain. An
252 average propagation velocity can be estimated from the slope coefficient of the regression
253 lines. For the selected flood events, the propagation velocities range between 6.7 m h^{-1}
254 and 11.5 m h^{-1}. It can be noted that the two largest floods present a similarly high
255 propagation velocity while the lowest flood is linked with the smallest propagation
256 velocity.

257

258 The relative homogeneity of hydraulic conductivities over the floodplain shows that the
259 spatial distribution of lag values over the study site cannot be caused by floodplain
260 morphology. Comparison of hydraulic conductivity values to the floodplain elevation
261 (Table 1) also shows that spatial distribution of hydraulic conductivities is not explained
262 by the floodplain morphology. Moreover, if direct groundwater recharge or hillslope
263 runoff processes were responsible for groundwater level fluctuations, a large variability
264 of lag values among piezometers would not be obtained for every flood event. Relations
265 between time lags and peak stream discharge values and between time lags and rising
266 limb times were investigated and no significant relationships emerged.

267

The high correlation values, the short positive time lags, and the increasing time lags with distance from the river observed from the cross-correlation analysis all suggest that piezometric levels in the floodplain are controlled by river stage fluctuations. However, this general pattern is variable in time and space. Figure 5 shows that there is a positive correlation between the time lag and the day of the year (DOY) on which the flood event occurred at four locations within the alluvial floodplain. The smallest time lags were recorded for the summer flood events (DOY 188 to 249). For all piezometers, a 50% increase in time lags between DOY 188 (7 July) and 336 (2 December) was observed. Although there is a general tendency to the increase of time lag throughout the summer, there is an opposite trend when several floods follow a period without precipitation event. Two "dry" periods occurred during this study, between DOY 205 and 230, and between DOY 250 and 320. For both periods, the first flood event has a significantly larger time lag and the time lag for each of the following storm events occurring after was relatively smaller. These "dry" periods resulted in a deeper unsaturated zone, which explain the significant increased time lags followed by decreased time lag.

The amplitude of groundwater fluctuations decreased with distance from the river (Figure 6). A damping effect can been seen, probably induced by the distance between the piezometer and the channel. All R^2 values are higher than 0.92. This amplitude variability is not related to floodplain morphology. Comparing the three flood events revealed that amplitudes conserve similar proportions, e.g., water level amplitudes recorded at 21 m distance were always 60% higher than amplitudes recorded 250 m from the channel, regardless of flood magnitude. In addition, the amplitudes of groundwater fluctuations close to the channel can be higher than the amplitudes of river stage

fluctuations. For example, 21 m from the channel, the 0.37 m river level fluctuation recorded during the 26 August–3 September event and the 1.04 m river level fluctuation recorded during the 5–12 September event induced groundwater fluctuations of 0.40 m (108%) and 1.14 m (109%), respectively. Also, comparison of the 26 August – 3 September event to 2–16 July event shows that a flood event of a lower magnitude (0.37 m) and of a shorter rising limb (32.5 h) induces larger water level fluctuations than a flood event of a higher magnitude (0.42 m) with a longer rising limb (90.8 h). The amplitudes of groundwater fluctuations depend not only on the piezometer-channel distance and on the magnitude of the flood events, but also on the duration of the flood rising limb.

3.2 Spatial analysis of groundwater level dynamics

At the study site, the Matane River is generally a gaining stream, i.e., the hydraulic gradient indicates that flow is towards the river. To investigate if the spatial dynamics of hydraulic gradients is affected during a flood event, hourly groundwater equipotential maps were produced. These maps suggest that hydraulic gradients vary temporally and spatially during flood events and that they may reverse. Figure 7 shows that the water pressure exerted on the channel banks from stream flooding induced hydraulic gradient to change flow orientation during the 5–12 September flood. At 22 $m^3 s^{-1}$ on 5 September at 00:00 am (Figure 7a), the Matane River was a gaining stream. The highest water level of 59.20 m at piezometer D223 and the lowest water level of 58.37 m at piezometer D21 indicate a west-oriented flow related to a hydraulic gradient of 3.31 mm m^{-1}. The hydraulic gradient indicated groundwater flow re-oriented towards the eastern valley

314 walls (Figure 7b) from 6 September 07:00 am (105 $m^3 s^{-1}$) to 11:00 pm (187 $m^3 s^{-1}$), even
315 if the peak stream discharge of 213 $m^3 s^{-1}$ was at 02:00pm. Using hydraulic heads from
316 piezometers D55 and D176, the steepest perpendicular hydraulic gradient obtained is
317 1.9 mm m^{-1} and been recorded at 3:15 pm on 6 September. The hydraulic gradient
318 returned to its initial orientation, i.e., gaining stream, at approximately 1:00pm on 7
319 September (Figure 7c). At that time, the hydraulic gradient between D223 and D21 was
320 2.81 mm m^{-1} and it is only on 8 September at 07:45 am that the hydraulic gradient at the
321 field site returned to its pre-storm condition of 3.31 mm m^{-1}.
322
323 Based on the highest saturated soil hydraulic conductivity (8.48×10^{-4} m s^{-1}, piezometer
324 D139 (table 1)), with the highest hydraulic gradient of 1.98 mm m^{-1} (observed at 3:15 pm
325 on 6 September), and a typical value of 0.25 for the effective porosity (Freeze and
326 Cherry, 1979), groundwater flow velocity through the floodplain during the inverted
327 hydraulic gradient was 2.41×10^{-2} m h^{-1}. However, cross-correlation analyses for the 5–12
328 September flood event indicate an average propagation velocity of 11.5 m h^{-1}, i.e., two to
329 three orders of magnitude higher than the estimated groundwater velocity. This suggests
330 that hydraulic head fluctuations correspond to the propagation of a groundwater
331 floodwave throughout the floodplain triggered by the river stage fluctuation. The 5–12
332 September 213 $m^3 s^{-1}$ flood event is the only recorded event that induced a change in
333 groundwater flow orientation of the alluvial aquifer during the study period. However, it
334 is expected that larger flood events would induce similar processes.
335

In order to evaluate the floodwave propagation through the Matane river alluvial aquifer, hydraulic heads profiles from the stream through a transect of piezometers (D21, D81, and D176) during the 5-12 September flood were assessed throughout the duration of the flood (Figure 8). River levels used for the profiles come from the river stage gauge downstream (RSGdn) temporal series. Results indicate that as the stage in the river increased, the flow direction in the aquifer reversed. At the start of the flood pulse, Matane river is a gaining stream. At the peak of the flood pulse on 6 September 04:00pm, the groundwater flow orientation was towards the valley wall, indicating that the river water level was higher than that of the alluvial aquifer. As the flood pulse receded, the groundwater flow direction reverted back towards the stream. It should also be noted, that as the river stage started to fall from 6 September 08:00pm to 7 September 04:00am, the underground floodwave was still propagating through the floodplain, hydraulic gradient was still reversed and hydraulic heads kept rising at D81 and D176. This would, first, inform that a floodwave may propagates beyond the study site (> 250 m from the river), but also highlight that the floodplain has stored water almost to the exfiltration of the water table at the floodplain surface at D176 (59.51 m (Table 1)). It is finally on 7 September at 08:00 am that both river stage and water levels were falling.

355

356 4. DISCUSSION

357 *4.1 Groundwater floodwave propagation*

358 This study highlights the effects of the Matane River discharge fluctuations on the water
359 level of its alluvial aquifer. Field measurements suggest that a floodwave propagates
360 through the gravelly floodplain over a spatial extent much larger than the hyporheic zone.
361 Results also suggest that the alluvial aquifer of the Matane Valley is hydraulically
362 connected and primarily controlled by river stage fluctuations, even at stream discharges
363 below bankfull. It has been reported that river stage fluctuations in some catchments were
364 the processes primarily responsible for groundwater fluctuations throughout a floodplain
365 (Lewandowski et al., 2009; Vidon, 2012). Another study reports that piezometers distant
366 from the channel reflect hillslope groundwater contributions (Jung et al., 2004). Here,
367 cross-correlation results (Figure 3b) show lower correlations and much longer delays
368 between precipitation and groundwater levels than between river levels and groundwater
369 levels. It is clear that direct precipitation contributes to recharge the unconfined alluvial
370 aquifer. However, this is not the primary process responsible for groundwater increases
371 during the flood events, probably because of the unsaturated storage capacity.
372 Lewandowski et al. (2009) showed that precipitation was responsible for 20% of the
373 groundwater fluctuations in the River Spree floodplain whereas, Vidon (2012) noted also
374 no significant correlation between precipitation and groundwater fluctuations,

375

376 The propagation of the hydraulic head fluctuations through alluvial aquifers during flood
377 events has been discussed by several authors (Sophocleous, 1991; Jung et al., 2004;

Lewandowski et al., 2009; Vidon, 2012). Jung et al. (2004) compared their results to a kinematic wave propagation based on flux velocities. This was done on a nearly synchronous response of the groundwater to the river stage during in-bank conditions, and on a wave-like response of the groundwater induced by an increase in river stage. Kinematic wave theory (see Lighthill and Withman, 1955) is based on the law of mass conservation through the continuity equation and a flux-concentration and may be applicable over a wide range of hydrological processes (Singh, 2002). To be considered as kinematic, a wave must be nondispersive and nondiffusive, two conditions that are necessary for the conservation of its length and amplitude over time and throughout space. In contrast, Thual (2008) showed that a dispersive and diffusive wave is considered as a dynamic wave. The amplitude of a dynamic wave will decrease over time and throughout space, but its length will increase.

In this study, the propagation of an underground floodwave, triggered by the river stage fluctuations for all flood events, is interpreted as a dynamic wave propagating within the alluvial aquifer. This interpretation is based on the non-conservation of hydraulic head fluctuations over time and through space. The groundwater response to the pulse induced by the rising river stage is however delayed and damped through the floodplain, as noted in Vekerdy and Meijjerink (1998) and Lewandowski et al. (2009). Figure 9 is a representation of a dynamic wave propagation through the alluvial aquifer of the Matane floodplain for the 5–12 September flood event. Near the river, hydraulic head amplitudes are high but the duration of high hydraulic heads is short. As a groundwater floodwave propagates distant from the river, friction through the porous medium causes a loss of

energy, which induces the damping effect. This damping effect causes water table amplitudes to become smaller, but hydraulic heads to remain high longer, inducing the floodwave crest to migrate (Figure 9). Every flood event, independent of its magnitude, induced dynamic wave propagations, but it is only the September event that caused hydraulic gradient to change flow orientation.

The groundwater floodwave hypothesis is also supported by the fact that a streamflood event induces water levels to rise instead of creating a lateral groundwater mass displacement through the floodplain. The absence of a significant displacement of river water in the floodplain during a flood event is supported by the propagation velocities of the 5–12 September flood event that are 2-3 orders of magnitude higher (6.00 to 10.93 m h^{-1}) than the groundwater velocity (10^{-2} m h^{-1}) measured at the highest reversed hydraulic gradient of the field site (1.9 mm m^{-1}) on 6 September at 3:15 pm. These results support those of Vidon (2012), who reported propagation velocities three orders of magnitude higher than groundwater velocities, which were in the range of 10^{-4} m h^{-1}. Jung et al. (2004) reported propagation velocities five to six orders higher than flux velocities of 10^{-4}-10^{-5} m h^{-1}, whereas Lewandowski et al. (2009) noted the propagation of pressure fluctuations approximately 1000 times faster than groundwater flow. Figure 5 shows an increase in the time lag throughout the year induced by a long period of groundwater discharging to the river between the 5–12 September and the 10–26 November flood events. This increase in the time lag represents not only a reduction of propagation velocities through the year, but also highlights the effects of prior unsaturated zone. Propagation velocities are not correlated with rainfall intensity. If

rainfall intensity affected time lags, a large variability of time lags between piezometers would not be observed at each flood event, nor would it be observed for similar rainfall intensities.

Streamfloods can affect the local groundwater flow directions in the floodplain depending on the flood magnitude. Potentiometric maps (Figure 7) show that the hydraulic gradient within the floodplain reversed at a stream discharge of 95 $m^3 s^{-1}$ during the 5–12 September flood event. Some researchers have reported reversed hydraulic gradients and the development of a groundwater ridge toward valley walls capable of 'swiching off' hillslope inputs during a streamflood with a stream discharge below bankfull, sometimes for long periods (e.g. Burt et al., 2002; Vidon, 2012). Here, the 5–12 September event is the only event that induced a groundwater flow reversal which lasted 16 h before returning to pre-storm initial hydraulic gradient three days later.

4.2 Groundwater flooding

The occurrence of groundwater flooding in floodplain environments is controlled by the degree of connectivity between a stream and its alluvial aquifer (Mardhel et al., 2007; Cobby et al., 2009). Figure 8 shows that groundwater levels rise almost synchronously as the river stage rises. But to determine the range of stream discharges at which exfiltration is likely to occur at study site, linear regression analyses for each piezometer were calculated using highest hydraulic heads reached below floodplain surface and the peak flow of recorded flood events (Figure 10a). Strong correlations ($R^2 > 0.96$) exist for all piezometers, taking account the 213 $m^3 s^{-1}$ event or not. For example, the 213 $m^3 s^{-1}$

447 during the 5–12 September event induced the hydraulic head to rise to 9 cm below the
448 surface at D176 and to 15 cm below the surface at D21 and D81. The hydraulic heads
449 rose closest to the floodplain surface at piezometers installed in the oxbow feature.
450 Figure 10b shows the spatial distribution of the predicted stream discharges producing
451 exfiltration at the study site. By extrapolating from the water level depths-flowrates
452 relations, it is possible to estimate that exfiltration would occur at stream discharges
453 ranging between 238 and 492 $m^3 s^{-1}$ depending on the location within the floodplain.
454 Figure 10b shows that the lowest predicted stream discharges would induce flooding at
455 the lowest part of the floodplain (i.e., in the oxbow), and at piezometers D55 and D175
456 only stream discharges higher than bankfull would induce exfiltration of the water table.
457 Estimated bankfull discharge of the Matane River is 350 $m^3 s^{-1}$, so according to the
458 models, exfiltration occurs at stream discharges well below bankfull. The range of stream
459 discharges that took place during the study period were all below the extrapolated
460 exfiltration thresholds supporting the fact that no exfiltration event was observed.
461 Although the exfiltration thresholds would need validation, the data strongly indicate that
462 river stage levels and underground floodwave propagation can contribute to groundwater
463 flooding. Further developments in the estimation of groundwater flooding river flow rates
464 should consider the initial hydraulic heads before stream floods occurred, the spatial
465 connectivity between piezometers by runoff at the floodplain's surface once exfiltration
466 occurred, or a possible overflow of the Matane River.

467

468 5. CONCLUSION

This study shows that water level fluctuations in the Matane alluvial floodplain are primarily governed by river stage fluctuations. The amplitudes of groundwater fluctuations depend on the distance from the channel, on the flood magnitude, and on the rising limb of the flood. The largest flood event recorded during the study period is the only event that influenced local groundwater flow orientation within the alluvial floodplain by generating an inversion of the hydraulic gradient toward the valley walls for sixteen hours. The results also show a damping effect of the groundwater response related to the distance of piezometers from the channel. Every flood event showed a large variability of lag values across the floodplain. The periods of groundwater discharging to the river of july and October 2011 caused time lags to increase for next flood events. Exfiltration of groundwater is predicted for stream discharges that can be well below bankfull. However, these estimations do not take into account the spatial connectivity between piezometers, the initial depth of the groundwater, or a possible overflow of the river. Finally, this study reveals that the pressure exerted on the river bank by a stream flood induces the propagation of a groundwater floodwave, interpreted as a dynamic wave, for all the studied floods. The propagation speed remains relatively constant across the floodplain but depends on the initial conditions within the floodplain. Propagation of groundwater level fluctuations occurs at every event, but only the largest event in this study affected groundwater flow directions. This study supports the idea that a river flood has a much larger effect in time and space than what is occurring within the channel. Further research including groundwater geochemistry would bring insights on energy exchange processes through the river bank and allow to determine whether and to what distance surface water reaches the floodplain below ground the during flood events.

492

493 ACKNOWLEDGEMENTS

494 This research was financially supported by the climate change consortium Ouranos as
495 part of the “Fonds vert” for the implementation of the Quebec Government Action Plan
496 2006-2012 on climate change, by BORÉAS, by the Natural Sciences and Engineering
497 Research Council of Canada (NSERC), by the Centre d’Études Nordiques, and by the
498 Fondation de l’UQAR. We are thankful to several team members of the Laboratoire de
499 recherche en géomorphologie et dynamique fluviale de l’UQAR for field assistance.

500

501

502 REFERENCES

503 Barlow, J.R., Coupe, R.H., 2009. Use of heat to estimate streambed fluxes during
504 extreme hydrologic events. Water Resour. Res. 45 (1), 1-10, doi: 566
505 10.1029/2007WR006121.

506 Burt, T.P., Bates, P.D., Stewart, M.D., Claxton, A.J., Anderson, M.G., Price, D.A., 2002.
507 Water table fluctuations within the floodplain of the River Severn, England. J. Hydrol.
508 262 (1–4), 1–20.

509 Cardenas, M.B., 2008. The effect of river bend morphology on flow and timescales of
510 surface water-groundwater exchange across pointbars. J. Hydrol. 362 (1–2), 134–141.

511 Cobby, D., Morris, S., Parkes, A., Robinson, V., 2009. Groundwater flood risk
512 management: advances towards meeting the requirements of the EU floods directive. J.
513 Flood Risk Manag. 2 (2), 111–119.

514 Freeze, R.A., Cherry, J.A., 1979. Groundwater. Prentice Hall, Englewood Cliff.

515 Gillham, R.W., 1984.The capillary fringe and its effect on water-table response. J.
516 Hydrol. 67, 307–324.

517 Gooseff, M.N., 2010. Defining hyporheic zones – Advancing our conceptual and
518 operational definitions of where stream water and groundwater meet. Geo. Compass 4
519 (8), 945–955.

520 Haycock, N.E, Burt, T.P., 1993. Role of floodplain sediments in reducing the nitrate
521 concentration of subsurface run-off : a case study in the Cotswolds, UK. Hydrol.
522 Processes 7, 287-295.

523 Hammer, Ø., Harper, D.A.T., Ryan, P.D., 2001. PAST: Paleontological statistics
524 software package for education and data analysis. Palaeontologia Electronica , 4 (1), 9.

525 Harvey, J.W., Bencala, K.E., 1993. The effect of streambed topography on surface–
526 subsurface water exchange in mountain catchments. Water Resour. Res. 29 (1), 89–98,
527 doi: 10.1029/92WR01960.

528 Harvey, J. W., J. D. Drummond, R. L. Martin, L. E. McPhillips, A. I. Packman, D. J.
529 Jerolmack, S. H. Stonedahl, A. Aubeneau, A. H. Sawyer, L. G. Larsen, and C. Tobias,
530 2012, Hydrogeomorphology of the hyporheic zone: Stream solute and fine particle
531 interactions with a dynamic streambed. J. Geo. Res. - Biogeosciences, Volume 117,
532 G00N11, doi:10.1029/2012JG002043.

533 Hvorslev, M.J., 1951. Time lag and soil permeability in groundwater observation. U.S.
534 Army Corps of Engineers, Waterways Experimental Station, Vicksburg, Miss., Bulletin
535 365.

536 Jung, M.T., Burt, T.P., Bates, P.D., 2004. Toward a conceptual model of floodplain water
537 table response. Water Resour. Res. 40 (12), 1–13.

538 Kreibich, H., Thieken, A., 2008. Assessment of damage caused by high groundwater
539 inundation. Water Resour. Res. 44 (9), W09409, doi:10.1029/2007WR006621.

Lebuis, J., 1973. Geologie du Quaternaire de la region de Matane-Amqui- Comtes de Matane et de Matapedia. Rapport DPV-216, Ministere des Richesses naturelles, Direction generale des Mines, Gouvernement du Quebec, Quebec, 18.

Lewandowski, J., Lischeid, G., Nützmann, G., 2009. Drivers of water level fluctuation and hydrological exchange between groundwater and surface water at the lowland river Spree (Germany): field study and statistical analyses. Hydrol. Processes 23 (15), 2117–2128.

Lighthill M.J., Whitham, G.B., 1955. On kinematic waves: 1. Flood movement in long rivers. Proceedings of the Royal Society London, Series A 229, 281–316.

Mardhel, V., Pinault, J.L., Stollsteiner, P., Allier, D., 2007. Etude des risques d'inondation par remontees de nappe sur le bassin de la Maine, Rapport 55562-FR, Bureau de recherches geologiques et minieres, 156.

Mertes, L.A., 1997. Documentation and significance of the perirheic zone on inundated floodplains. Water Resour. Res. 33 (7), 1749–1762.

Pinault, J.L., Amraoui, N., Golaz, C., 2005. Groundwater-induced flooding in macropore-dominated hydrological system in the context of climate changes. Water Resour. Res. 41 (5), 1–16.

Singh, V.P., 2002. Is hydrology kinematic? Hydrol. Processes, 16 (3), 667–716.

Sophocleous, M.A., 1991. Stream-floodwave propagation through the great bend alluvial aquifer, Kansas: Field measurements and numerical simulations. J. Hydrol. 124 (3–4), 207–228.

561 Stonedahl, S.H., Harvey, J.W., Wörman, A., Salehin, M., Packman, A.I., 2010. A
562 multiscale model for integrating hyporheic exchange from ripples to meanders. Water
563 Resour. Res. 46, 1–14, doi:10.1029/2009WR008865.

564 Thual, O., 2008. Propagation de l'onde de crue, in Thual, O. (Ed.), Hydrodynamique de
565 l'Environnement. Les Editions de l'Ecole Polytechnique, Toulouse, pp.131-157.

566 Triska, F.J., Kennedy, V.C., Avanzio, R.J., Zellweger, G.W., Bencala, K.E., 1989.
567 Retention and transport of nutrients in a third-order stream in northwestern California:
568 Hyporheic processes. Ecology, 70 (6), 1893–1905.

569 Vekerdy, Z., Meijerink, A.M.J., 1998. Statistical and analytical study of the propagation
570 of flood-induced groundwater rise in an alluvial aquifer. J. Hydrol., 205 (1–2), 112–125.

571 Vidon, P., 2012. Towards a better understanding of riparian zone water table response to
572 precipitation: surface water infiltration, hillslope contribution or pressure wave
573 processes? Hydrol. Processes, 26 (21), 3207–3215.

574 Woessner, W., 2000. Stream and fluvial plain interactions: rescaling hydrogeologic
575 thought. Groundwater, 38 (3), 423–429.

576 Wondzell, S.W., Gooseff, M.M., 2013, Geomorphic controls on hyporheic exchange
577 across scales: watersheds to particles, in Shroder, J. F. (Ed.), Treatis in Geomorphology.
578 Academic Press, San Diego, pp. 203-218.

579

Figures captions Cloutier et al.

Figure 1: (A) Location of the the Matane River Basin, Quebec, Canada; (B) Location of the study site within a coarse sand gravelly floodplain constructed by fluvial dynamics; (C) Position of the piezometers within the study site. Piezometers with pressure sensors are indicated. The names of the piezometers reflect the perpendicular distance to the Matane River.

Figure 2: Water levels and river stage time series from 21 June to 12 December 2011.

Figure 3: Cross-correlation functions using river levels as input and groundwater levels as output (solid lines) and precipitation as input and groundwater levels as output (dashed lines).

Figure 4: Time lags of piezometers as a function of distance from the river for three selected flood events.

Figure 5: Time lags as a function of day of the year of flood occurrence at four selected positions within the alluvial floodplain.

Figure 6: Water level fluctuations within the floodplain for three flood events. Values parenthesis indicate duration of flood pulse rising limb and flood even magnitude.

Figure 7: Groundwater flow directions suggested from the equipotential lines during 5–12 September event.

Figure 8: Propagation of a groundwater floodwave within the aquifer during the 5–12 September flood event. Solid lines indicate rising river stage and water levels and dashed lines indicate falling river stage and water levels . ** maximum river stage.

601

602 Figure 9: Floodwave propagation within the floodplain for the 5–12 September 213 $m^3 s^{-1}$
603 flood event using the standardized water level from pieozometers D21, D55, D81, D127,
604 D175, D223 and D257. Step time is hourly from 6 September, 00:00 am. The black line
605 represents the groundwater floodwave crest displacement.

606 Figure 10: Predicted stream discharges for exfiltration. (a) Regression model of predicted
607 exfiltration discharge for selected piezometers; (b) spatial distribution of the predicted
608 exfiltration discharges. Regression dashed lines correspond to extrapolation. Vertical
609 dashed line correspond to Matane river bankfull discharge.

610

611

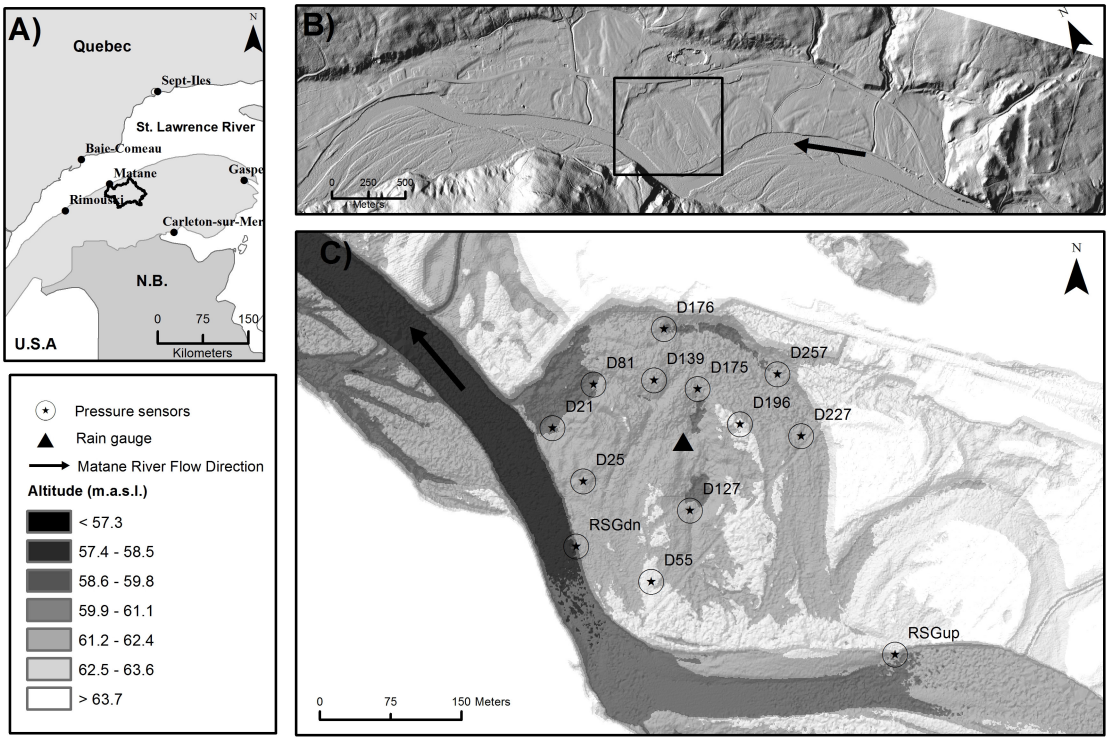

612

613

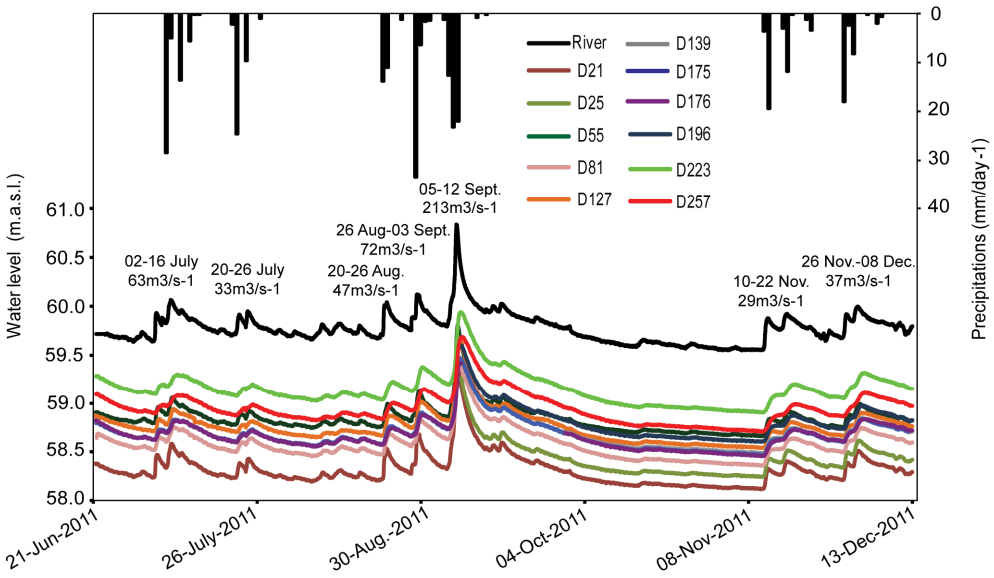

614

615

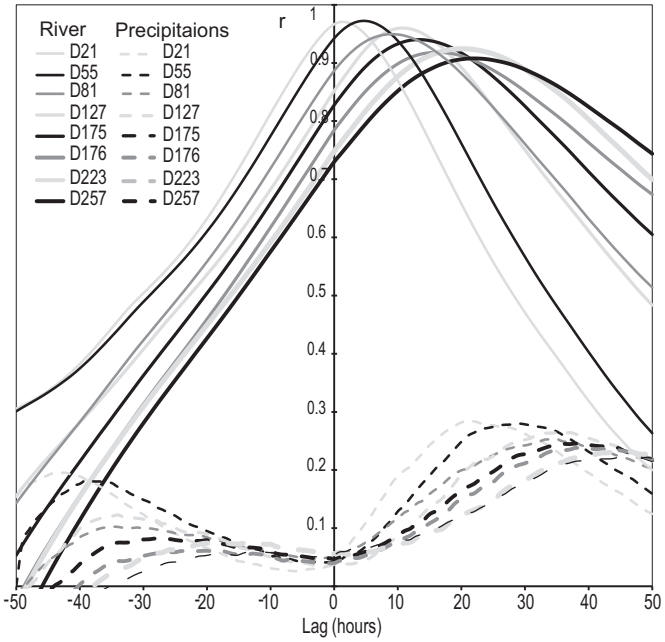

616

617

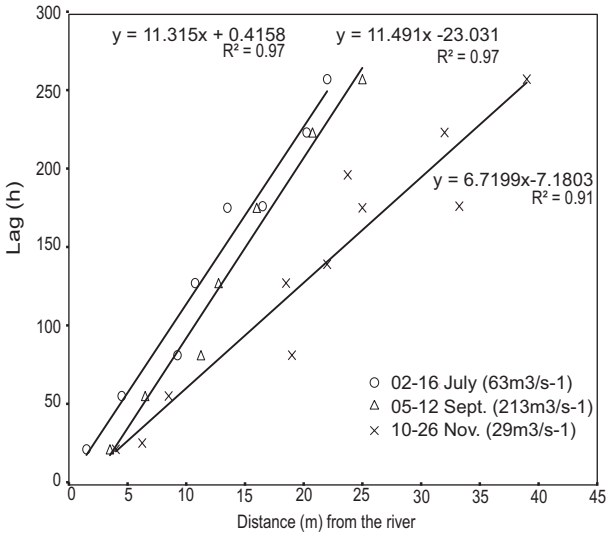

618

619

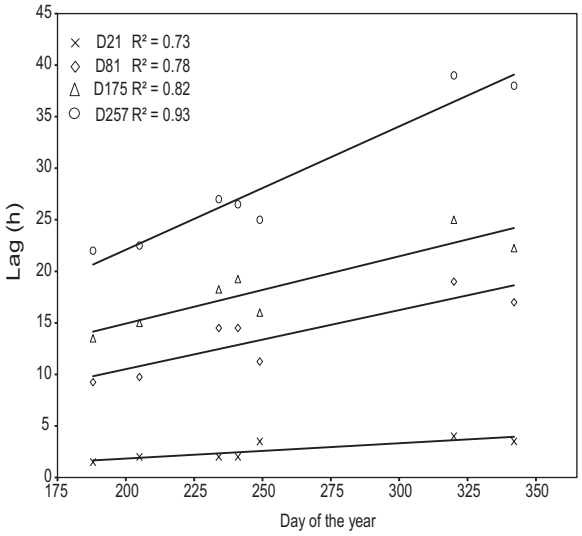

620

621

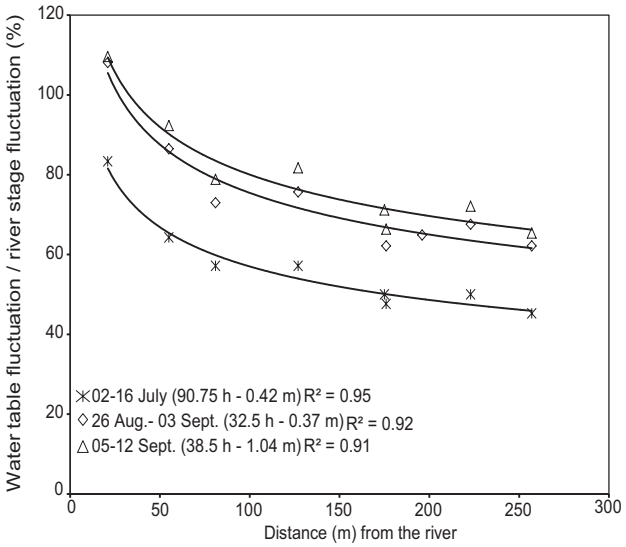

622

623

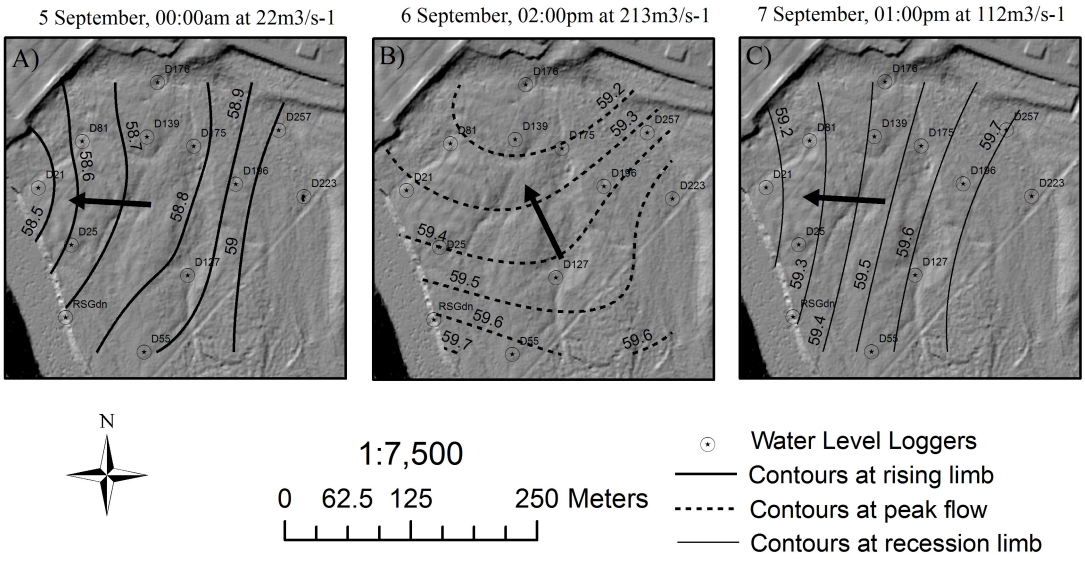

624

625

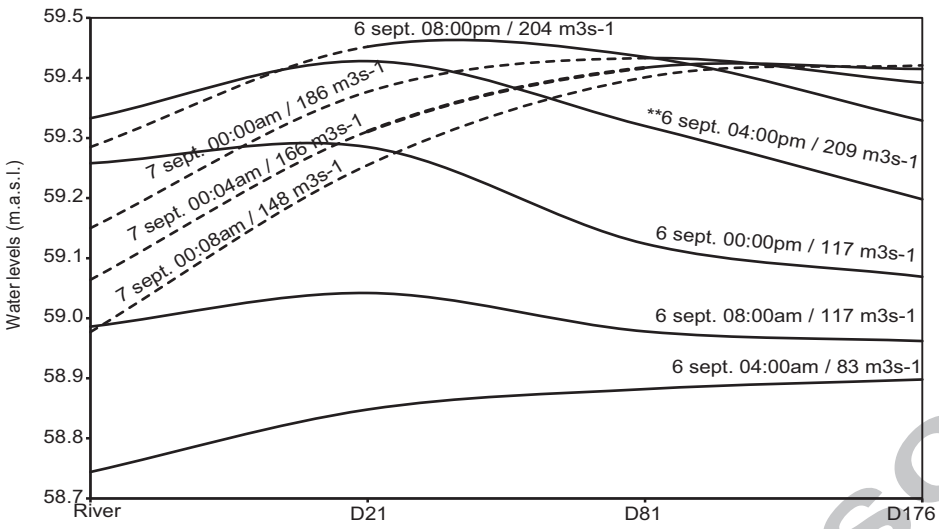

626

627

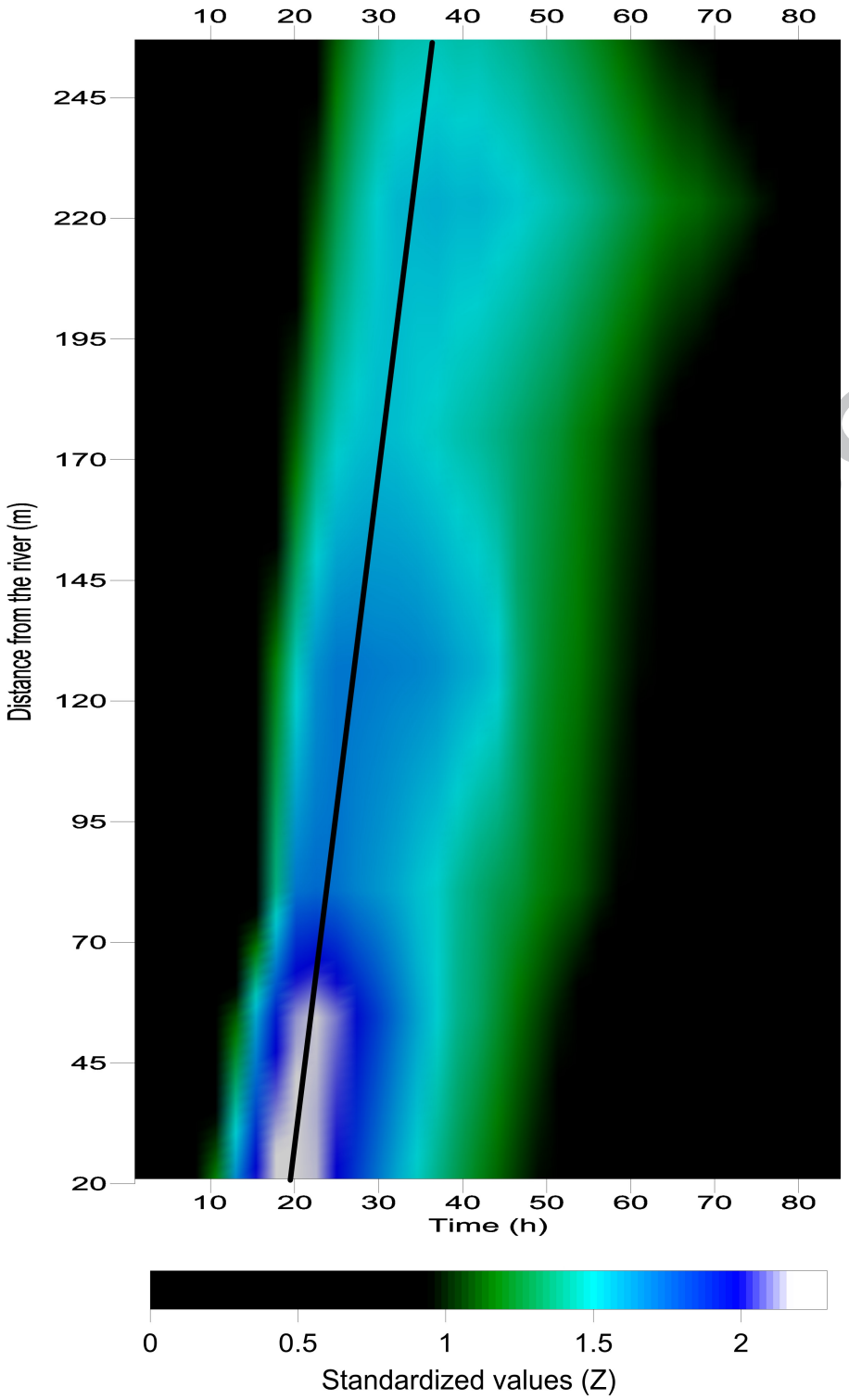

628

629

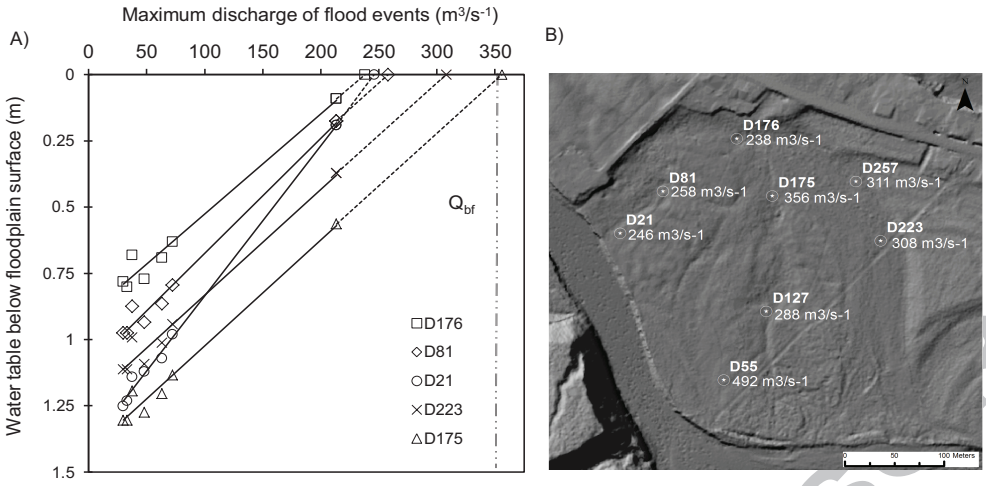

630

631

632 **Table 1:** Hydraulic conductivity values derived from slug tests.

Piezometer	Floodplain elevation (m)	K (m s^{-1})
D21	59.65	1.99×10^{-4}
D25	60.55	1.94×10^{-4}
D55	61.17	2.78×10^{-4}
D81	59.61	6.61×10^{-4}
D139	60.82	8.48×10^{-4}
D175	60.03	6.18×10^{-4}
D176	59.51	2.10×10^{-5}
D196	61.03	1.95×10^{-4}
D223	60.31	2.07×10^{-4}
D257	60.02	8.90×10^{-5}

633

634

635

636 Key Points:

637 • A groundwater floodwave can propagate through an alluvial aquifer

638 • Streamfloods affect groundwater flow orientation

639 • Streamfloods leading to groundwater exfiltration

640

641